Significant inter-annual fluctuation in CO2 and CH4 diffusive fluxes from subtropical aquaculture ponds: implications for climate change and carbon emission evaluations

Significant inter-annual fluctuation in CO_2 and CH_4 diffusive fluxes from subtropical aquaculture ponds: Implications for climate change and carbon emission evaluations

Ping Yang [a,b,c,d], Linhai Zhang [a,b,c], Yongxin Lin [a,b,c], Hong Yang [e,f], Derrick Y.F. Lai [g], Chuan Tong [a,b,d], Yifei Zhang [a], Lishan Tan [g], Guanghui Zhao [a], Kam W. Tang [h]

a. School of Geographical Sciences, Fujian Normal University, Fuzhou, 350007, PR China

b. Key Laboratory of Humid Subtropical Eco-geographical Process of Ministry of Education, Fujian Normal University, Fuzhou, 350007, PR China

c. Fujian Provincial Key Laboratory for Subtropical Resources and Environment, Fujian Normal University, Fuzhou, 350117, PR China

d. Research Centre of Wetlands in Subtropical Region, Fujian Normal University, Fuzhou, 350007, PR China

e. Department of Geography and Environmental Science, University of Reading, Reading, UK

f. College of Environmental Science and Engineering, Fujian Normal University, Fuzhou, 350007, China

g. Department of Geography and Resource Management, The Chinese University of Hong Kong, Shatin, New Territories, Hong Kong SAR, China

h. Department of Biosciences, Swansea University, Swansea, SA2 8PP, UK

Abstract

Aquaculture ponds are potential hotspots for carbon cycling and emission of greenhouse gases (GHGs) like CO_2 and CH_4, but they are often poorly assessed in the global GHG budget. This study determined the temporal variations of CO_2 and CH_4 concentrations and diffusive fluxes and their environmental drivers in coastal aquaculture ponds in southeastern China over a five-year period (2017–2021). The findings indicated that CH_4 flux from aquaculture ponds fluctuated markedly year-to-year, and CO_2 flux varied between positive and negative between years. The coefficient of inter-annual variation of CO_2 and CH_4 diffusive fluxes was 168% and 127%, respectively, highlighting the importance of long-term observations to improve GHG assessment from aquaculture ponds. In addition to chlorophyll-*a* and dissolved oxygen as the common environmental drivers, CO_2 was further regulated by total dissolved phosphorus and CH_4 by dissolved organic carbon. Feed conversion ratio correlated positively with both CO_2 and CH_4 concentrations and fluxes, showing that unconsumed feeds fueled microbial GHG production. A linear regression based on binned (averaged) monthly CO_2 diffusive flux data, calculated from CO_2 concentrations, can be used to estimate CH_4 diffusive flux with a fair degree of confidence ($r^2 = 0.66$; $p < 0.001$). This algorithm provides a simple and practical way to assess the total carbon diffusive flux from aquaculture ponds. Overall, this study provides new insights into mitigating the carbon footprint of aquaculture production and assessing the impact of aquaculture ponds on the regional and global scales.

Keywords

Greenhouse gases; Diffusive flux; Carbon footprint; Climate impact; Aquaculture ponds

Graphical abstract

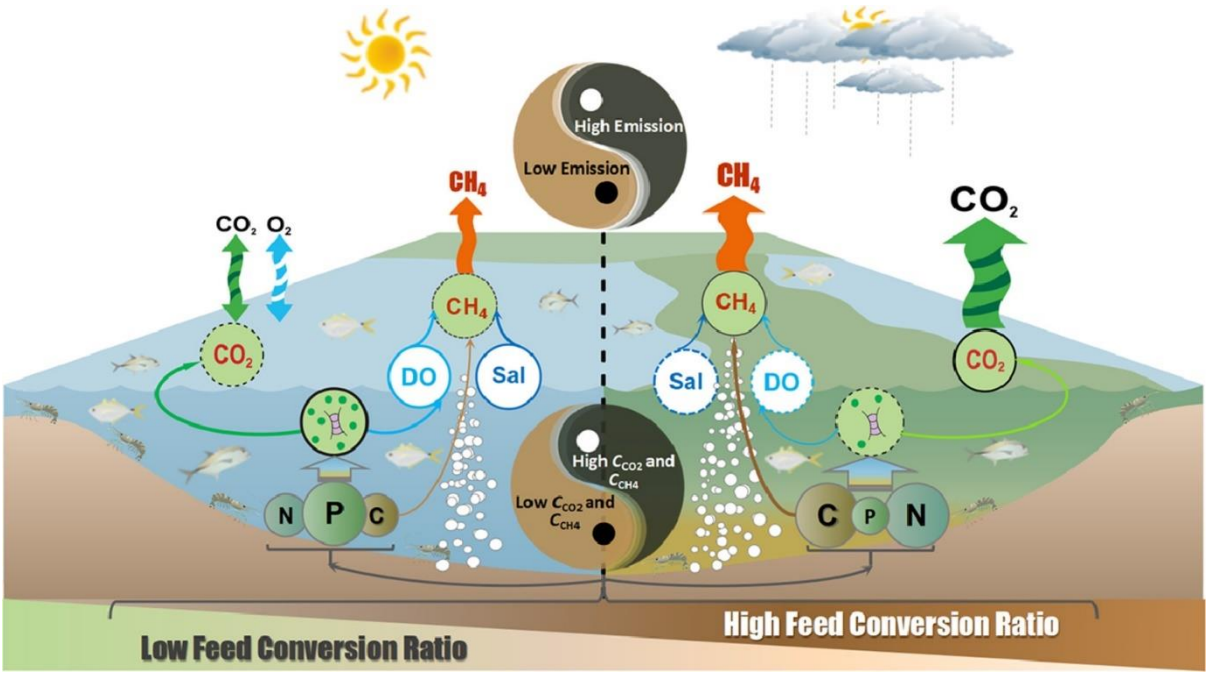

1. Introduction

Methane (CH_4) and carbon dioxide (CO_2) are the two primary greenhouse gases (GHGs), together contributing over 80% of the total atmospheric radiative forcing (Friedlingstein et al., 2022; Le Quéré et al., 2018; Myhre et al., 2013). In 2023, the atmospheric CO_2 and CH_4 concentrations have reached 420 ppm and 1900 ppb, respectively (National Oceanic and Atmospheric Administration, 2023), which is approximately 48% and 156% over the pre-industrial values. To mitigate global carbon emission, China has pledged to cap its carbon emission by 2030 and achieve net-zero emission by 2060 (Yang et al., 2022a). However, identifying the sources and quantifying the magnitude of GHG emissions are crucial for predicting and reducing GHG emissions (Borges et al., 2015; Jia et al., 2022; Yang et al., 2023a).

Carbon emissions from inland aquatic ecosystems such as lakes, rivers and reservoirs have been quite well studied (Bastviken et al., 2011; Raymond et al., 2013; Wang et al., 2019), but emissions from small and shallow ponds (<0.001km^2) are still poorly quantified and are often excluded from the global GHG budget (Holgerson, 2015; Holgerson and Raymond, 2016). There are estimated 3.2 billion small ponds globally (Downing, 2010), covering a total area of ~0.8 million km^2 (Holgerson and Raymond, 2016). Due to their relatively high organic loading (Rubbo et al., 2006), these ponds can be hotspots for carbon cycling (Holgerson, 2015) and GHG emissions (e.g., Jensen et al., 2023; Peacock et al., 2021; Prėskienis et al., 2021). Among the small ponds, aquaculture ponds are of particular interest thanks to the fast-growing aquaculture sector world-wide (Naylor et al., 2021). In aquaculture ponds, the persistent introduction of fertilizers, animal wastes and feeds can significantly elevate the production and release of GHGs, a phenomenon not often observed in natural ponds (Boyd et al., 2010; Chanda et al., 2019; Tong et al., 2020).

Approximately 25,700 km^2 in China is occupied by aquaculture ponds (Chen et al., 2015, 2016), and about 60% of them are concentrated in estuaries and coastal bays (Duan et al., 2020). Most of them are small-hold aquaculture farms that are subject to fluctuations in ambient conditions (e.g., air temperature, sunlight, precipitation) and different farming practices (Chen et al., 2016; Kosten et al., 2020; Yang et al., 2023b), leading to considerable variations in GHG production and emissions from the ponds (e.g., Dong et al., 2023a; Liu et al., 2016; Zhao et al., 2021). As the two major carbon-based GHGs, the dynamics of CO_2 and CH_4 are controlled by different organisms and biological processes: CO_2 is consumed by photoautotrophs via photosynthesis and produced by heterotrophs via respiration (Gudasz et al., 2010; Liu et al., 2010), whereas methanogenesis is largely driven by methanogens in the anoxic sediment (Lin and Lin, 2022; Segers, 1998; Gruca-Rokosz et al., 2020), with some contribution from the water-column (Bogard, et al., 2014; Tang et al., 2016). On the other hand, the two gases are connected within the carbon cycle, e.g., organic carbon can feed into both respiration and methanogenesis; CH_4 and CO_2 can also be interconverted by methanotrophs and methanogens, respectively, under specific conditions (Chowdhury and Dick, 2013; Zabranska and Pokorna, 2018). Therefore, we may expect some empirical relationships between the two gases in aquaculture ponds.

Due to logistical limitations, researchers usually make measurements at low frequency (once a month or less) and for a short duration (no more than two years). This may not be sufficient to reveal the temporal variations in GHG emissions. Given the sheer number of small-hold aquaculture ponds in China, it is impractical for officials to monitor them all. Proper assessment of GHG emissions may therefore require self-monitoring and reporting by the farmers, but the farmers usually lack the time, skills or equipment to do rigorous gas measurements. Between the two gases, CO_2 can be measured relatively easily using inexpensive sensors

(e.g., Zosel et al., 2011). By developing simple algorithms to estimate CH_4 from CO_2 data, we can greatly expand the nation's ability to assess the combined carbon emission from the fast-growing aquaculture sector.

In this study, we measured the concentrations of dissolved CO_2 and CH_4 in the water column of aquaculture ponds in southeastern China over five years between 2017–2021, from which we calculated the diffusive flux of CO_2 and CH_4 across the air-water interface. The objectives were to determine the magnitude and temporal variations of CO_2 and CH_4 concentrations and diffusive fluxes and the key environmental drivers. We then examined the empirical relationships between CO_2 and CH_4 by binning the data at different temporal resolutions, in order to derive useful algorithms for assessing GHG outputs from aquaculture ponds.

2. Materials and methods

2.1. Study areas

Measurements and sample collections took place in the Shanyutan Wetland, located within the Min River estuary in the Fujian province, China (26°00′36″–26°03′42″N, 119°34′12″–119°41′40″E, Fig. 1). The region is characterized by a subtropical marine monsoon climate typical of the southern regions, with an average yearly temperature of 19.6°C and an annual precipitation of approximately 1,350 mm (Yang et al., 2020a). In this region, the prevalent plant species include the indigenous *Phragmites australis* and *Cyperus malaccensis*, along with the non-native *Spartina alterniflora* (Gao et al., 2019; Tong et al., 2018). Over the past decades, extensive areas of the tidal saltmarshes have been transformed into aquaculture shrimp ponds. The aquacultural production period is typically from May to November, with one crop of shrimp (*Litopenaeus vannamei*) produced per year. Previous research provides comprehensive information on the aquaculture ponds and associated farming techniques (Tong et al., 2020).

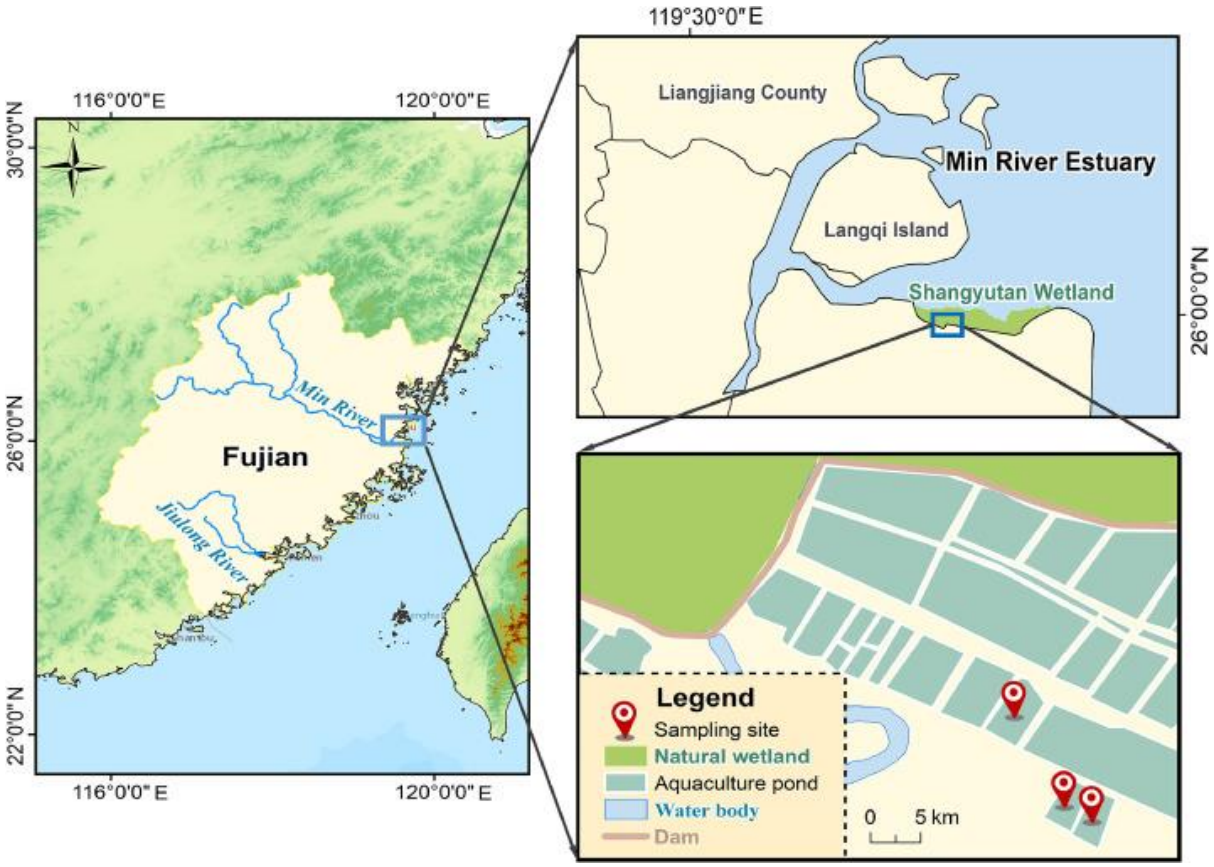

Fig. 1. Locations of the study areas and sampling sites in Shanyutan Wetland within the Min River Estuary, Fujian Province, southeast China.

2.2. Collection of water samples

Three shrimp ponds were sampled 1–3 times each month between 2017 and 2021. In each pond, water samples from 20-cm depth were collected using an organic glass hydrophores at three different sites (Tian et al., 2023; Yang et al., 2020b). Subsequently, the water was poured into 150-mL polyethylene bottles and into 55-mL pre-weighed serum glass bottles. Before the bottles were sealed, a 0.2 mL saturated $HgCl_2$ solution was added to halt microbial processes (Borges et al., 2018; Marescaux et al., 2018). A total of 648 water samples were obtained and promptly transported to the laboratory in ice coolers within 4-6 h.

2.3. Measurement of dissolved gas concentrations

The levels of dissolved CO_2 (C_{CO2}) and CH_4 (C_{CH4}) in the water samples were measured with the headspace equilibration method (Yang et al., 2019; Zhang et al., 2021). Briefly, water samples without bubble were gathered in 55 mL serum glass bottles that had been pre-weighed. In the laboratory, a headspace was formed by injecting 25 mL of ultrahigh purity nitrogen (N_2) gas (99.999%) into each glass bottle. Afterwards, the bottles were vigorously shaken in an oscillator (IS-RDD3, China) for 10 min to attain equilibrium between the atmospheric and water phases (Cotovicz Jr et al., 2016). Following a 30-minute settling period, a 5-ml sample of the headspace was extracted and injected into a Shimazu GC-2010 gas chromatograph (Kyoto, Japan) equipped with a flame ionization detector (FID) to measure CO_2 and CH_4. Five standards CO_2 (or CH_4) gas, namely 50 (2), 100 (8), 500 (500), 3000 (1000) and 10,000 (10,000) ppm, were used to calibrate the FID.. Using the specific water and headspace volumes in the glass bottles, along with the solubility coefficient of CO_2 (or CH_4) for the specific temperature and salinity, the *in situ* C_{CO2} (or C_{CH4}; μmol L^{-1}) was calculated (Wanninkhof, 1992).

2.4. Calculations of diffusive GHG fluxes

Diffusive fluxes of CO_2 (F_{CO2}; mmol m^{-2} h^{-1}) and CH_4 (F_{CH4}; μmol m^{-2} h^{-1}) across the air-water interface were determined based on Equation 1 (Cotovicz Jr et al., 2016; Jia et al., 2022; Musenze et al., 2014):

$$F_{gas} = k_x \times (C_w - C_{eq}) \quad (1)$$

where F_{gas} was the diffusive flux of CO_2 (or CH_4); C_W was the concentrations of dissolved CO_2 (or CH_4) (μmol L^{-1}) in the surface water; C_{eq} was the concentration of CO_2 (or CH_4) (μmol L^{-1}) at equilibrium with the overlying atmosphere at the *in situ* conditions. The coefficient for gas exchange k_x (cm h^{-1}) was calculated as (Crusius and Wanninkhof, 2003):

$$k_x = \left[2.07 + \left(0.215 \times U_{10}^{1.7}\right)\right] \times \left(\frac{Sc_{gas}}{600}\right)^{-n} \quad (2)$$

where $U_{10}^{1.7}$ was the wind speed without friction (m s^{-1}) measured at a height of 10 m above the aquatic surface (Crusius and Wanninkhof, 2003); n was the proportionality coefficient, which depended on $U_{10}^{1.7}$ (if $U_{10}^{1.7}$ > 3 m s^{-1}, then n = 1/2; if $U_{10}^{1.7} \leq$ 3 m s^{-1}, then n = 2/3) (Cole and Caraco, 1998). Sc_{gas} was the Schmidt number of CO_2 (or CH_4) calculated from Eq. (3) and Eq. (4);

$$Sc_{CO2} = 2073.1 - 125.62t + 3.6276t^2 - 0.043219t^3 \quad (3)$$

$$Sc_{CH4} = 2039.2 - 120.31t + 3.4209t^2 - 0.040437t^3 \quad (4)$$

where t was the surface water temperature (°C).

The calculated CH_4 flux was converted to CO_2-equivalent flux based on the conversion factor of 45 for a 100-year time horizon (Neubauer and Megonigal, 2019), and added to the calculated CO_2 emission to determine the total CO_2-equivalent emission.

2.5. Ancillary environmental variables

During each sampling campaign, *in situ* measurements were taken at a water depth of 20 cm at each location. These measurements included water temperature (T_W), pH, salinity and dissolved oxygen (DO) using a portable pH/Temperature meter (IQ150, USA), a Eutech Instruments-Salt6 salinity meter (USA) and a 550A YSI multiparameter probe (Yellow Springs, OH, USA). The MRE weather station provided data on meteorological variables, such as air temperature (T_A), wind speed (W_S) and air pressure (A_P), measured with the Vantage Pro 2 automatic meteorological station (Hayward, CA, USA).

In the laboratory, we filtered the water samples through 0.45-μm acetate fiber membranes. Subsequently, we measured the filtrates for their content of dissolved organic carbon (DOC) with a TOC-$_{VCPH/CPN}$ Analyzer (Shimadzu, Japan), and total dissolved phosphorus (TDP) and total dissolved nitrogen (TDN) with a flow injection analyzer (Skalar Analytical SAN^{++}, Netherlands). Chlorophyll-*a* (Chl-*a*) was extracted in 90% ethanol (or acetone) in darkness for 24 h and then measured on a Shimadzu UV-2450 UV–visible spectrophotometer (Kyoto, Japan) (Kang et al., 2023; Xu et al., 2017). Feed conversion ratio of the farmed organisms was determined by dividing the total dry feed weight provide by the overall weight increase (Zhang et al., 2018).

2.6. Statistical analysis

Before conducting statistical tests, we assessed the data for normal distribution. The coefficient of variation for CO_2 (or CH_4) fluxes were determined by dividing the standard deviation by the average value. The effect of sampling years on environmental factors, concentrations of dissolved GHGs, and diffusive fluxes was evaluated using a one-way ANOVA in IBM's SPSS 22.0 software (Armonk, NY, USA). To assess the relationships between environmental factors and dissolved GHG concentrations or diffusive fluxes, we employed the Spearman correlation method, using the vegan package in R Version 4.1.0 (R Foundation for Statistical Computing, 2013), and redundancy analysis (RDA) using the software CANOCO version 5.0 (Microcomputer Power, Ithaca, NY, USA). Partial least square structural equation modeling (PLS-SEM) was conducted in R Version 4.1.0 (R Foundation for Statistical Computing, 2013) with the 'semPLS' package to evaluate the direct or indirect effect of environmental variables on the GHGs. More details of the PLS-SEM analysis can be found in Tan et al. (2022, 2023).

To derive predictive relationship between CO_2 concentration (or diffusive fluxes) and CH_4 concentration (or diffusive fluxes), we ran linear regressions through the data at different resolutions: raw data without binning; binning (averaging) data by months, by seasons and by year. We compared the regression outputs and considered an r^2 value of > 0.5 to be suitable for applications. For all statistical analyses, a significance threshold of $p < 0.05$ was used.

3. Results

3.1. Physico-chemical properties and feed conversion ratio

The physico-chemical properties of the pond's surface water are shown in Fig. 2. There were significant between-year differences in all of the variables. T_W averaged ~28°C in 2017-2018, but was significantly lower in 2019-2021 (Fig. 2a). Salinity was at 3.5 ‰ in the first two years, then increased significantly in 2019 and again in 2020 (Fig. 2b). Water pH was between 8.75 and 9.25, except in 2019 when it dropped to 7.5 (Fig. 2c). Mean DO was > 6 mg L^{-1} with higher concentrations in 2018 and 2020 (Fig. 2d).

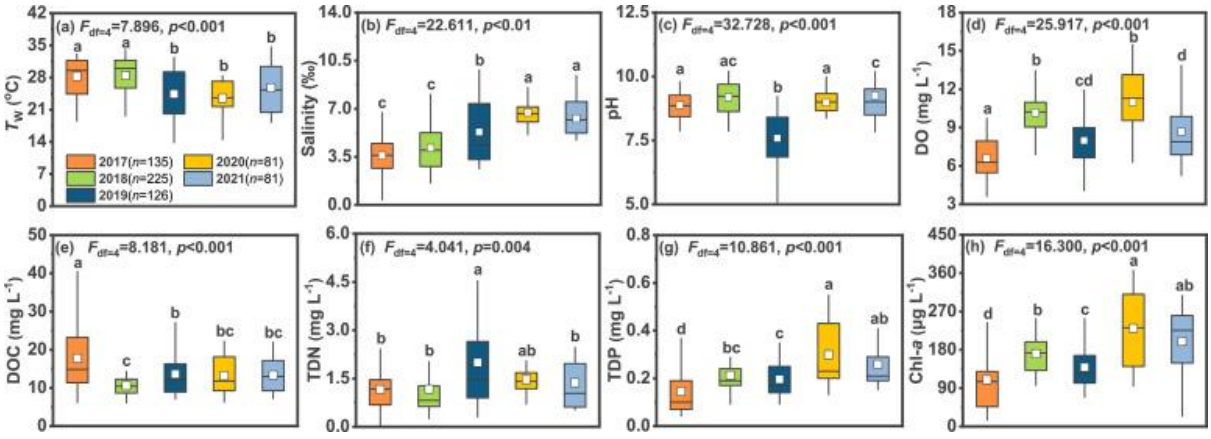

Fig. 2. Box plots of (a) water temperature (T_W), (b) salinity, (c) pH, (d) dissolved oxygen (DO), (e) dissolved organic carbon (DOC), (f) total dissolved nitrogen (TDN), (g) total dissolved phosphorus (TDP) and (h) chlorophyll-*a* (Chl-*a*) in surface water for coastal aquaculture ponds over a five-year period. Different letters above the boxes indicate significant differences (p<0.05).

DOC ranged from 10.6 to 17.7 mg L^{-1}, with a significantly higher concentration in 2017 (Fig. 2e). TDN varied between 1.2 and 2.0 mg L^{-1}, and was significantly higher in 2019 (Fig. 2f). TDP and Chl-*a* exhibited similar temporal variations over the five-year period: lowest in 2017 and highest in 2020 (Figs. 2g,h).

Feed conversion ratio varied significantly over time, with the highest value of 1.9 in 2017, followed by 1.5 in 2019, 1.3 in 2020, 1.1 in 2021, and 0.7 in 2018 (Figure S1).

3.2. Inter-annual variations in GHG concentrations and fluxes

C_{CO2} and F_{CO2} varied significantly between years (p<0.001; Fig. 3). The highest annual mean C_{CO2} was 37.4 ± 2.6 µmol L^{-1} in 2017, and the lowest at 10.9 ± 0.9 µmol L^{-1} in 2017 (Fig. 3a). F_{CO2} ranged from -0.12 ± 0.03 mmol m^{-2} h^{-1} in 2020 to 1.3 ± 0.2 mmol m^{-2} h^{-1} in 2017 (Fig. 3b). C_{CH4} varied significantly between 0.48 ± 0.06 µmol L^{-1} and 4.3 ± 0.8 µmol L^{-1} across the years (p<0.001; Fig. 3c). F_{CH4} also varied significantly with time, between 15.0 to 153.7 µmol m^{-2} h^{-1} (p<0.001; Fig. 3d).

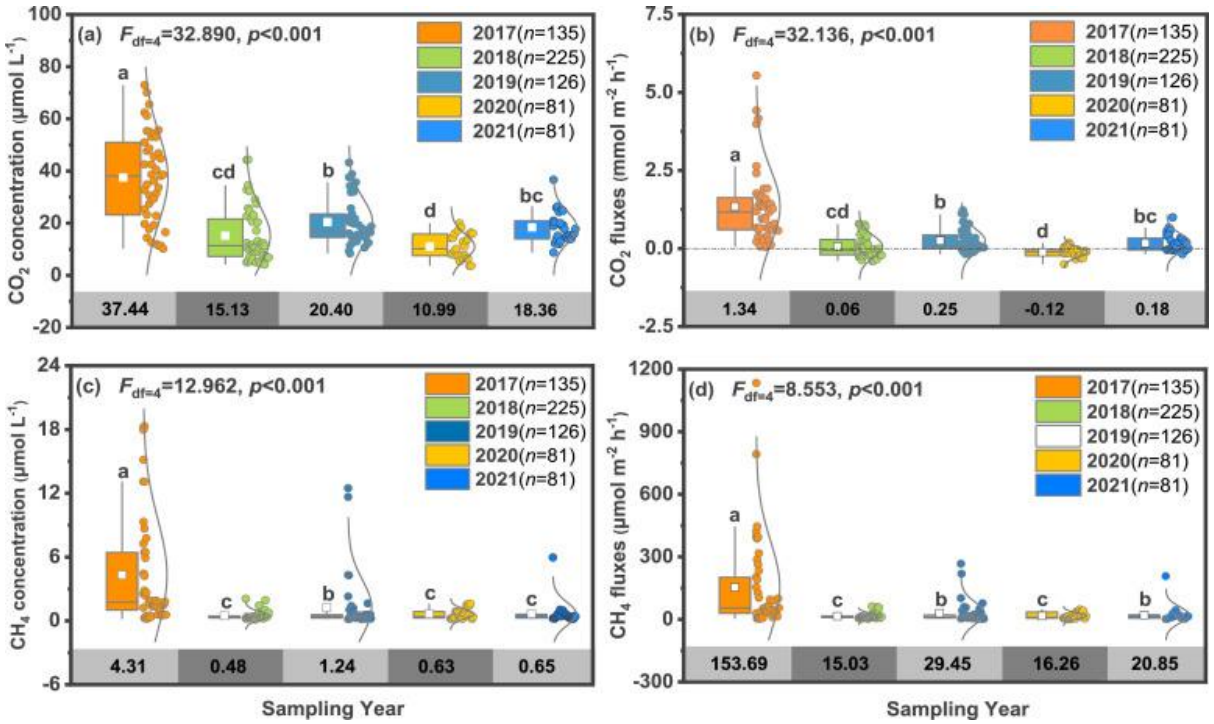

Fig. 3. Box plots of dissolved GHG concentrations in surface water and diffusive GHG flux across water-air interface for coastal aquaculture ponds over a five-year period. Different letters above the boxes indicate significant differences (p<0.05).

The combined CO_2-eq diffusive flux showed significant variations over time (Fig. 4), and the coefficient of variation was 133.9%. Over the five-year period, the mean combined diffusive flux ranged from 28.9 ± 5.3 to 695.9 ± 152.4 kg CO_2-eq ha^{-1} yr^{-1} (Fig. 4), with an average value of 206.8 ± 123.9 kg CO_2-eq ha^{-1} yr^{-1}. CH_4 accounted for over 70% of the combined CO_2-eq diffusive flux in each year.

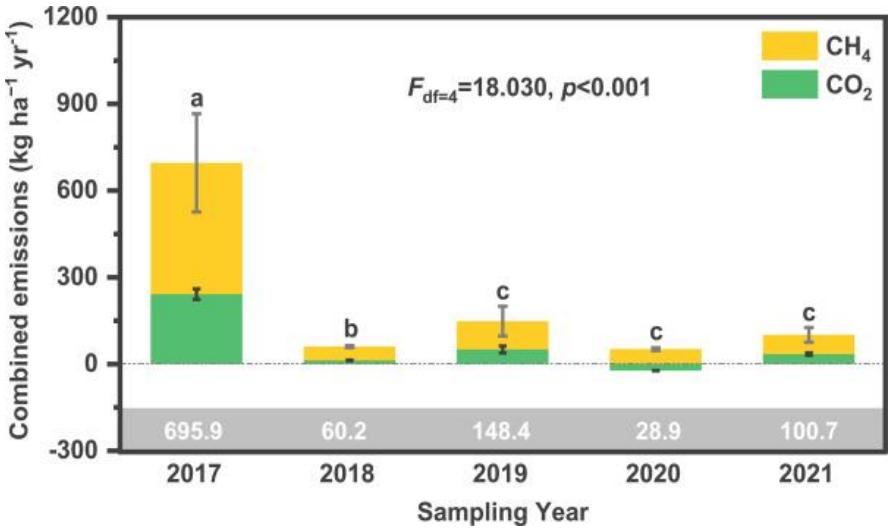

Fig. 4. Inter-annual variability in combined CO_2-equivalent emissions from the coastal aquaculture ponds during the farming period between 2017 and 2021.

3.3. Environmental drivers of GHG concentrations and diffusive fluxes

According to Spearman correlations (Figure S2) and RDA analysis (Fig. 5), the inter-annual variations in C_{CO2} and F_{CO2} were strongly driven by Chl-*a*, DO and TDP, which together explained 79.5% of the variations. The inter-annual variations in C_{CH4} and F_{CH4} were primarily determined by DOC, Chl-*a* and DO, which together explained 93.7% of the variations.

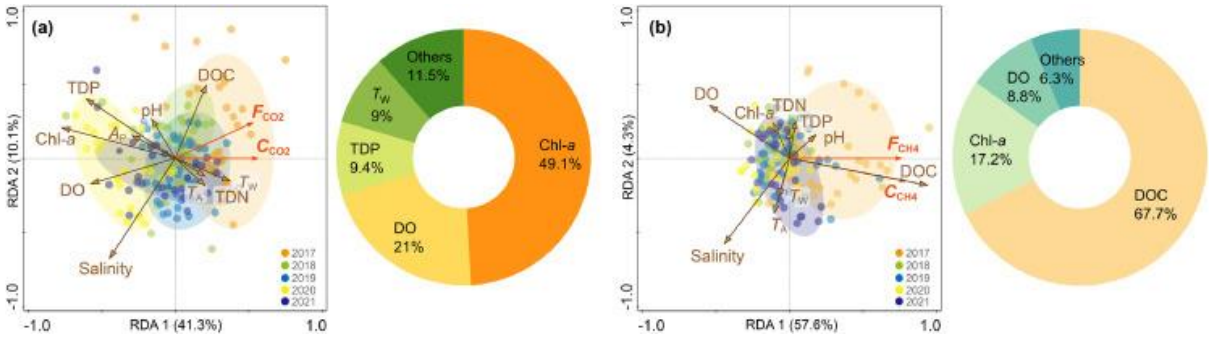

Fig. 5. Results of redundancy analysis (RDA) of (a) dissolved CO_2 concentration (C_{CO2}) [or CO_2 diffusive fluxes (F_{CO2}) across the water-air interface], and (b) dissolved CH_4 concentration (C_{CH4}) [or CH_4 diffusive fluxes (F_{CH4}) across the water-air interface], showing the loadings of the different environmental variables. The pie charts show the percentages of variance in CO_2 flux (or CO_2 concentration) and CH_4 flux (or CH_4 concentration) explained by the different variables. See main text for explanation of the abbreviations.

Based on PLS-SEM analysis, Chl-*a*, DO and TDP all had a direct negative effect on C_{CO2}, which in turn affected F_{CO2} (Fig. 6a). DO also had a direct negative effect on F_{CO2}. TDP positively influenced Chl-*a*, which in turn had a positive effect on DO. C_{CH4} was affected positively by DOC and negatively by Chl-*a* and DO; these then indirectly affected F_{CH4} (Fig. 6b). Salinity had a negative effect on DOC and F_{CH4}.

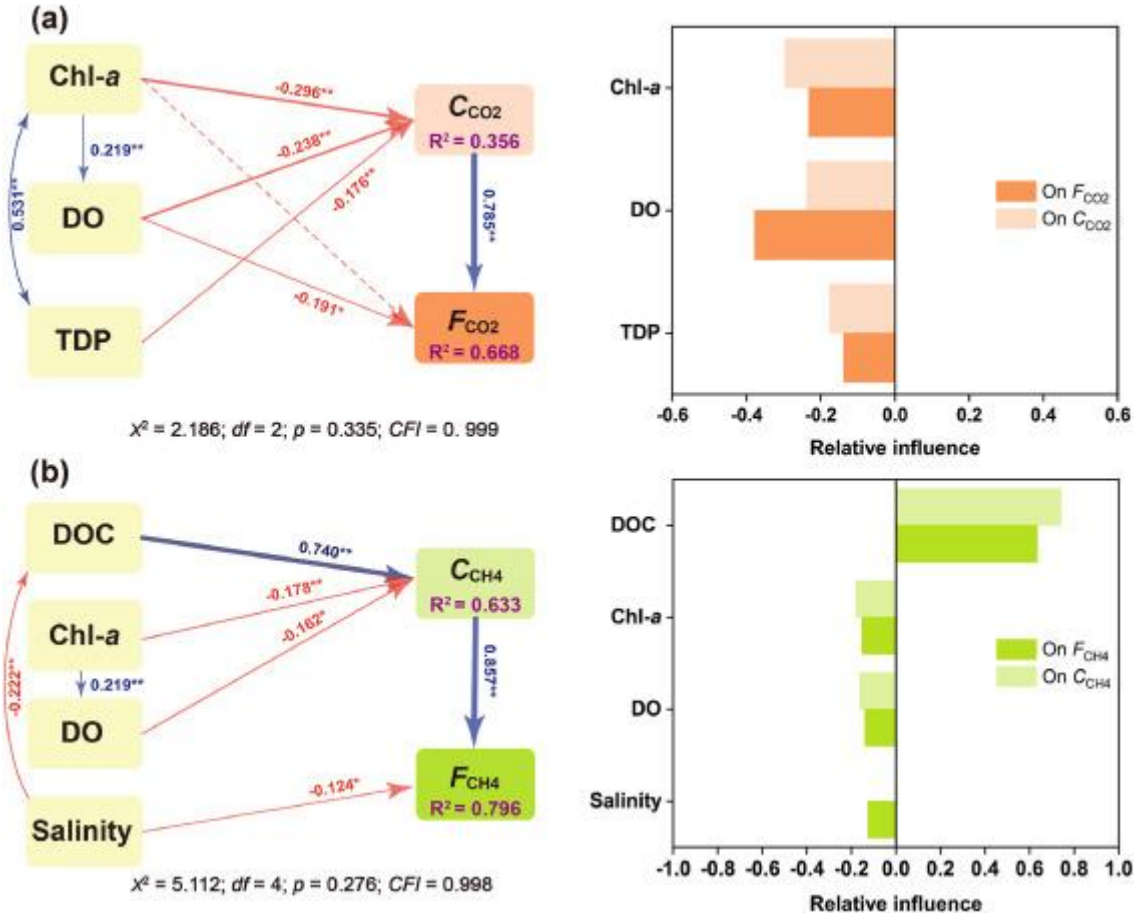

Fig. 6. Partial least square structural equation modeling (PLS-SEM) to evaluate the direct and indirect effects of environmental factors on (a) dissolved CO_2 concentration (C_{CO2}) and CO_2 diffusive fluxes (F_{CO2}) across the water-air interface, and (b) dissolved CH_4 concentration (C_{CH4}) and CH_4 diffusive fluxes (F_{CH4}) across the water-air interface. Solid blue and red arrows indicate significant positive and negative effects, respectively, and dotted arrow indicates insignificant effect on the dependent variable. Numbers adjacent to arrows are standardized path coefficients, indicating the effect size of the relationship. R^2 represents the variance explained for target variables. * $p < 0.05$; ** $p < 0.01$.

3.4. Predictive relationships between CO_2 and CH_4

We ran linear regressions using CO_2 concentration (or flux) as the independent variable and CH_4 concentration (or flux) as the predicted variable. We started with raw data without binning, then gradually decreased the resolution by binning (average) the data by month, season or year (Fig. 7). With raw data, the relationship was not significant for concentration, but it was significant for flux despite the very low r^2 value (Table 1). By binning the data, the regressions were all significant and the r^2 value increased. The r^2 value for concentration data was lower than 0.5 in all but the lowest resolution (yearly average), whereas the r^2 value for flux data was at 0.66 or higher (Table 1).

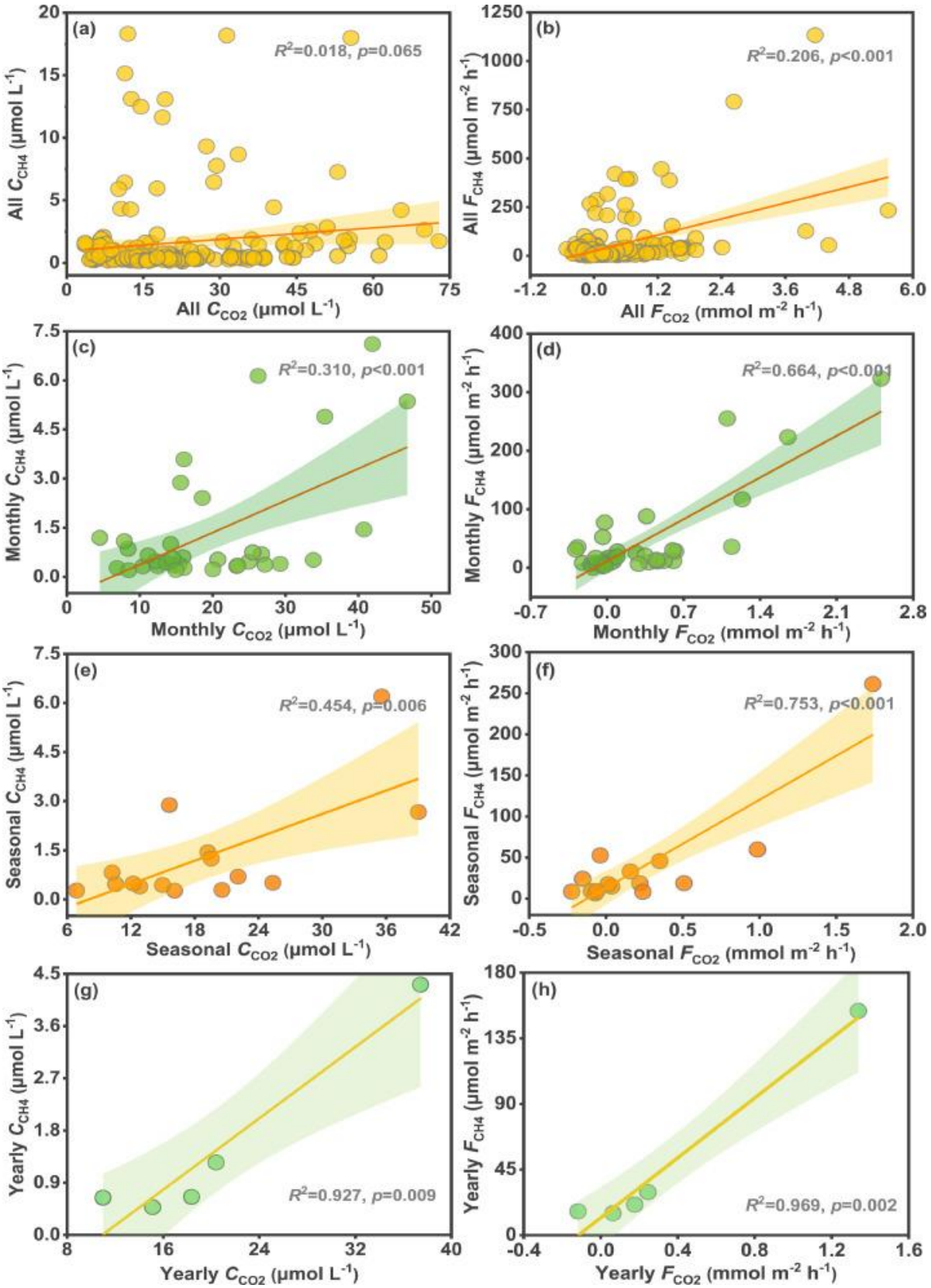

Fig. 7. Linear regressions between C_{CO2} (or F_{CO2}) and C_{CH4} (or F_{CH4}) using all data without binning, and data binned (averaged) by month, by season or by year. Output parameters of the regression analysis are listed in Table 1.

Table 1. Linear regression analysis with CO_2 concentration (C_{CO2}; μmol L^{-1}) or flux (F_{CO2}; mmol m^{-2} h^{-1}) as independent variable (x); CH_4 concentration (C_{CH4}; μmol L^{-1}) or flux (F_{CH4}; μmol m^{-2} h^{-1}) as predicted variable (y). Regressions were run using all data without binning, data binned (averaged) by month, by season or by year. Outputs include y-intercept, slope, standard error of slope, r^2 and p values of the regressions.

x	*y*	Intercept	Slope	Slope SE	r^2	*p*
All data						
C_{CO2}	C_{CH4}	0.969	0.030	0.016	0.018	0.065
F_{CO2}	F_{CH4}	25.293	68.279	9.869	0.206	0.000
Monthly						
C_{CO2}	C_{CH4}	-0.605	0.098	0.025	0.310	0.000
F_{CO2}	F_{CH4}	11.782	101.848	12.428	0.664	0.000
Seasonal						
C_{CO2}	C_{CH4}	-0.959	0.119	0.036	0.454	0.006
F_{CO2}	F_{CH4}	13.064	107.174	17.016	0.753	0.000
Yearly						
C_{CO2}	C_{CH4}	-1.681	0.154	0.025	0.927	0.009
F_{CO2}	F_{CH4}	11.973	102.653	10.609	0.969	0.002

4. Discussion

4.1. Effects of feed conversion ratio

In aquaculture, feeds are applied to sustain the animals (Avnimelech and Ritvo, 2003; Chen et al., 2016; Pouil et al., 2019), but only a small fraction of these feeds is effectively transformed into biomass (Flickinger et al., 2020; Molnar et al., 2013; Sahu et al., 2013). The efficiency at which the animals utilize the feeds is expressed as feed conversion ratio (FCR = amount of feed/amount of biomass produced). In this study, we found that FCR varied significantly between years (Figure S1), which may be a result of variable survival and physiological state of the farmed animals, or quality of the feeds. FCR correlated positively with DOC and negatively with DO (Fig. 8), suggesting that unconsumed feeds were decomposed into dissolved organics that subsequently fueled microbial respiration, as supported by the positive correlations between FCR and C_{CO2} and F_{CO2} (Figs. 9a and 9b). Unconsumed feeds and other organic wastes could also accelerate methane production, as shown by the positive correlations of FCR with C_{CH4} and F_{CH4} (Figs. 9c and 9d).

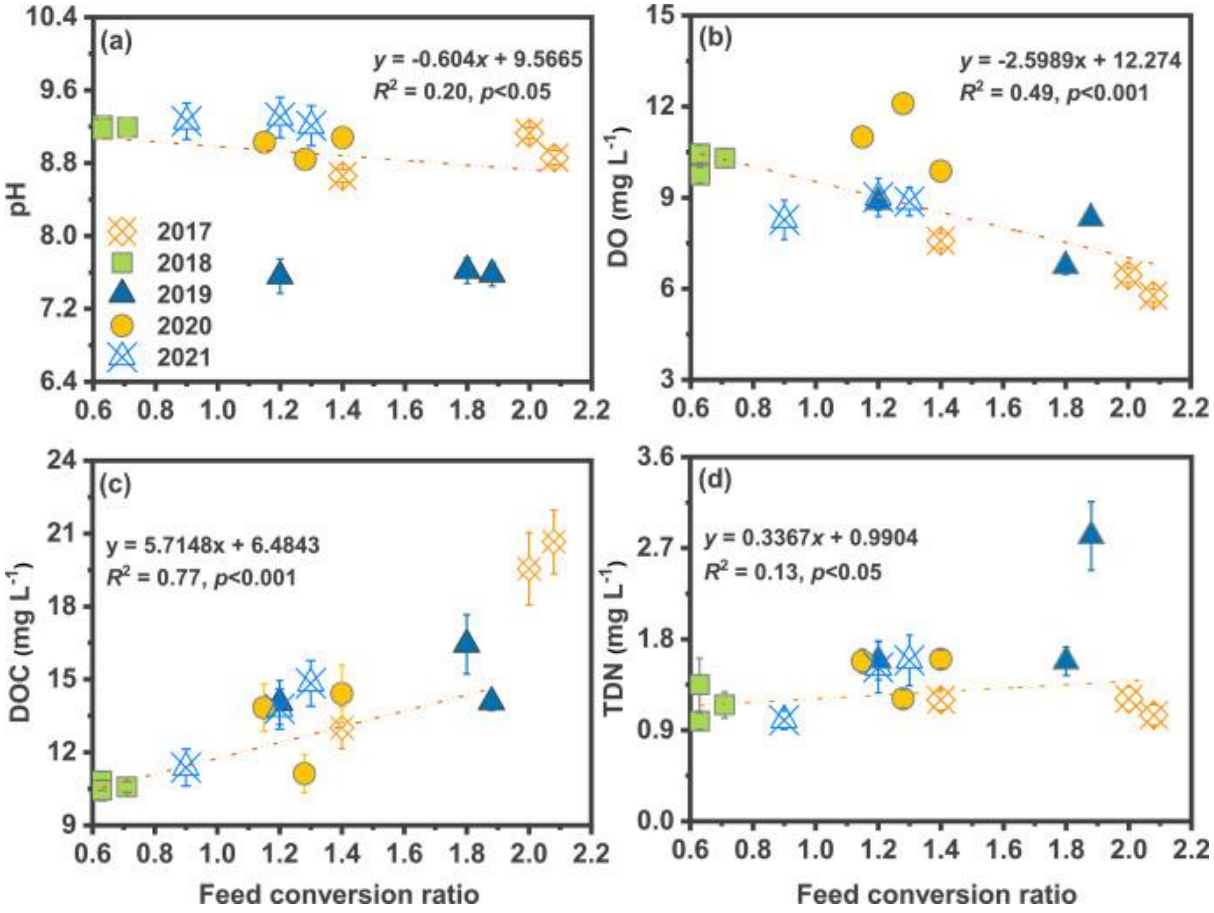

Fig. 8. Linear relationship between pH, DO, DOC, TDN and feed conversion rate (FCR) in coastal aquaculture ponds over a five-year period. Parameter bounds on the regression coefficients are 95% confidence limits. Feed conversion rate = dry weight of feeds added / wet weight of shrimps produced.

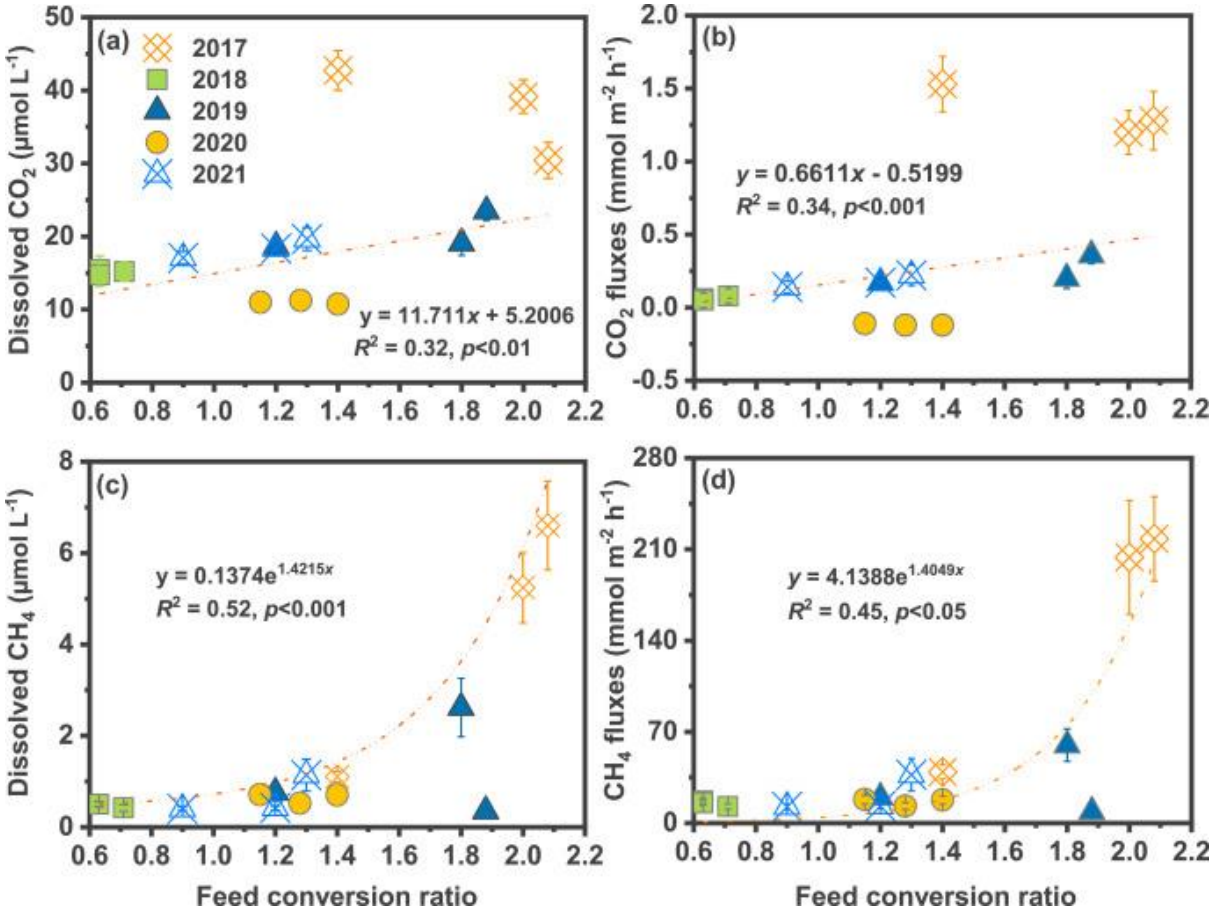

Fig. 9. Relationship between dissolved CO_2 concentration, diffusive CO_2 flux and feed conversion rate (a, b), and between dissolved CH_4 concentration, diffusive CH_4 flux and feed conversion rate (c, d) in coastal aquaculture ponds over a five-year period. Parameter bounds on the regression coefficients are 95% confidence limits.

4.2. Environmental drivers of CO_2

The surface-water CO_2 concentration exhibited remarkable variations across the five-year period and the aquaculture ponds switched between being a source and a sink of CO_2 to the atmosphere (Figs. 3a and 3b). CO_2 was consumed via photosynthesis by microalgae, as indicated by the significant negative correlation between Chl-*a* and C_{CO2} and F_{CO2} (Figure S2a). Microalgal biomass in the aquaculture ponds was regulated by dissolved nutrients such as TDP but not TDN (Figure S2a). This may be attributed to the high TDN (1.2~2.0 mg L^{-1}; Fig. 2f) and low TDP (0.1~0.3 mg L^{-1}; Fig. 2g) concentrations resulting in a strong P-limitation (Bernhard and Peele, 1997; Lapointe et al., 2015). The key role of TDP in regulating CO_2 was also confirmed by PLS-SEM analysis (Fig. 6a).

Our correlation (Figure S2a) and RDA (Fig. 5a) analyses showed that water temperature (T_W) was an important driver of C_{CO2} and F_{CO2}. The inter-annual variability in T_W in the ponds was approximately 5°C, with considerably lower values in 2017 and 2018. Not only that higher water temperature would increase the system respiration and DOC mineralization, but it may also decrease photosynthetic CO_2 uptake by negatively impacting Chl-*a* (Figure S2a). Together, this would increase CO_2 concentration and flux (Gudasz et al., 2010; Xiao et al., 2020; Huttunen et al., 2003).

4.3. Environmental drivers of CH_4

The average concentrations of dissolved CH_4 in the ponds was 800–8,000% saturated relative to the atmosphere, making the ponds a net source of CH_4 to the air (Fig. 3), similar to others inland aquatic ecosystems (Borges et al., 2015; Natchimuthu et al., 2016; Praetzel et al., 2021). The very high C_{CH4} in the aquaculture ponds could be attributed to the high DOC loading (Fig. 5b), likely from unconsumed feeds and animal wastes (Figure 8; Yang et al., 2020b), which fueled CH_4 production (Berberich et al., 2020; Davidsonet al., 2018; Zhou et al., 2018). This was further supported by the significant correlation found (1) between feed conversion rate and DOC concentrations (p<0.001; Fig. 8c), and (2) between DOC and dissolved CH_4 concentrations (or CH_4 fluxes) (p<0.001; Figs. 5b and S2b).

Salinity is another factor that governs CH_4 dynamics in coastal habitats (Segarra et al., 2013; Poffenbarger et al., 2011; Vizza et al., 2017). Higher salinity favors sulfate reducing bacteria over methanogens (Neubauer et al., 2013; Chambers et al., 2013; Vizza et al., 2017), resulting in a lower CH_4 emission (Poffenbarger et al., 2011; Welti et al., 2017; Wilson et al., 2015). Consistent with these earlier observations, during the five-year period of our study, 2017 saw the highest CH_4 diffusive flux, while 2018, 2020 and 2021 recorded reduced fluxes (Fig. 3d), which corresponded to the interannual rise in salinity of the pond water (Fig. 2b) as a result of decline in precipitation (Figure S3). The key role of salinity in regulating CH_4 was also confirmed by our PLS-SEM analysis (Fig. 6b).

Dissolved oxygen often determines the balance between CH_4 production and CH_4 oxidation (Bastviken et al., 2008; Liu et al., 2016; Schrier-Uijl et al., 2011). We observed substantial interannual variations in DO (Fig. 2d) that mirrored the variations in Chl-*a* (Fig. 2h), and DO had strong negative effects on C_{CH4} and F_{CH4} (Figs. 6b and S2b), suggesting that photosynthetic oxygen production facilitated methane oxidation in the water column.

4.4. Implications for carbon emission assessments and caveats

The escalating need worldwide for protein from aquatic sources has driven the fast expansion of aquaculture ponds, particularly in developing nations (Duan et al., 2020; FAO, 2017; Luo et al., 2022), but aquaculture also causes environmental problems such as nutrient pollution and GHG emissions (Dong et al., 2023b; MacLeod et al., 2020; Yuan et al., 2019). In order to assess the climate impact of coastal aquaculture ponds, we calculated the CO_2+CH_4 combined CO_2-equivalent diffusive flux, which averaged 1,908 ± 721 kg CO_2-eq ha^{-1} yr^{-1}, substantially higher than the average value from China's reservoirs and lakes (Li et al., 2018) and elsewhere (Deemer et al., 2016; Bastviken et al., 2011). Although CH_4 flux (Fig. 3d) was lower than CO_2 flux (Fig. 3b) in absolute term, the much higher warming potential of CH_4 meant that it accounted for much of the combined CO_2-eq emission (Fig. 4). This is different from the result of an earlier meta-analysis, which shows a CO_2:CH_4 flux (CO_2-eq) ratio of > 1 for small ponds (Holgerson and Raymond, 2016). The difference may be explained by the fact that aquaculture ponds are more eutrophic than natural ponds, which tends to favor methanogenesis and increase CH_4 emission. Extrapolating our data to all aquaculture ponds in the coastal region of China (total 1.5×10^4 km^2; Duan et al., 2020), we estimated that the combined CO_2-equivalent emissions from these ponds would be equivalent to ~1.5% of the national terrestrial biosphere carbon sink in China (–2,419 Tg CO_2-eq yr^{-1}; Wang et al., 2020).

Hence, harmonizing economic growth, food security and GHG mitigation from aquaculture systems presents a significant challenge. From our research data, it is evident that the diffusive fluxes of CO_2 and CH_4 from coastal aquaculture ponds decreased with the decline in FCR (Figs. 9b and 9d). Enhancing feed utilization efficiency through better feed formulation and

management may be pivotal in minimizing GHG emissions from aquaculture ponds, thereby promoting an eco-friendly and sustainable production.

In the global effort to combat climate change, proper assessment of GHG emissions from all sectors is required. Although diurnal and seasonal variations of carbon emission from aquaculture ponds have been investigated (e.g., Hu et al., 2020; Yuan et al., 2021; Zhang et al., 2022), most of the studies were limited to a relatively short time period. Our measurements over the five-year period (2017–2021) showed large inter-annual variations, with the coefficient of variation for CO_2 and CH_4 fluxes at 168.0% and 127.3%, respectively. Therefore, short-term or low-frequency measurements could result in large accounting errors in GHG budget.

This creates a conundrum for national GHG assessment. Because of the sheer number of small-hold aquaculture ponds spreading over nearly the entire coastline of China, the government simply does not have the resource to monitor them frequently and will have to rely on the farmers to report data on a regular basis, but sophisticated and expensive equipment and procedures are not suitable for small-hold aquaculture operators. Therefore, simple and practical methods for estimating GHG emissions will be highly desirable. Automated or handheld dataloggers for dissolved CO_2 are relatively inexpensive and low maintenance (e.g., Zosel et al., 2011), and F_{CO2} can be calculated from C_{CO2} using easily obtained wind (from weather station) and water temperature data (stand-alone sensor or integrated into CO_2 sensor). We therefore attempted to derive useful algorithms to predict F_{CH4} from F_{CO2}, and compared the outcomes by binning the data at different time resolutions.

Using only the raw data, the linear regressions had poor predictive power ($r^2 < 0.5$), suggesting that CO_2 and CH_4 dynamics in the aquaculture ponds were regulated by different factors there were loosely coupled in time. However, the predictive power of the algorithms improved considerably when we used data averaged by month, by season and by year (Table 1), suggesting that the biogeochemical processes for CO_2 and CH_4 were more in-sync at the lower temporal resolutions. For applications, we recommend measuring C_{CO2} in high frequency, from which F_{CO2} can be calculated, then binning F_{CO2} by month to preserve more temporal detail in the data (Fig. 7); monthly F_{CH4} can then be derived from the algorithm with a fair degree of confidence ($r^2 = 0.664$; $p < 0.001$).

Although the algorithm should provide a simple and reliable way to assess total diffusive carbon emission from aquaculture ponds, it is important to consider that this approach did not take into account CH_4 ebullition from the sediment, which at times can be a much larger emission source than diffusion (Yang et al., 2022b). However, ebullition is highly heterogenous in time and in space (de Mello et al., 2018; Martinez and Anderson, 2013; Yang et al., 2020b); it cannot be characterized by conventional water sampling or *in situ* sensors, and proper measurement would require frequent deployment of gas trap (Yang et al., 2020b) or hydroacoustic detector (Martinez and Anderson, 2013), both of which are not practical for farmers. Devising a simple and reliable method to estimate CH_4 ebullition from aquaculture ponds remains a key challenge to assessing the true extent of climate footprint of the sector.

5. Conclusions

In 2019, the worldwide aquaculture output amounted to 116.8 million tons. FAO (2020) forecasts a 32% surge by 2030, which intensifies concerns about the impact on pollution and climate (Chen et al., 2023; IPCC, 2019). It is a delicate task to balance between economic development, food security and GHG mitigation in the aquaculture sector.

Several studies have shown that artificial aeration is a simple and effective method to decrease CH_4 emission from aquaculture ponds, although its adoption among farmers remains limited (Fang et al., 2022; Yang et al., 2023b). We propose that improving feed formulation and refining feed strategies can not only decrease FCR but also cut down carbon emission, leading to a more profitable and sustainable production.

This study showed that coastal aquaculture ponds were a strong source for atmospheric CO_2 and CH_4 but with significant temporal variations. As such, short-term or low-frequency measurements may result in erroneous GHG budget. We produced a simple algorithm to derive monthly CH_4 diffusive flux from CO_2 concentration measurements, the latter of which can be monitored routinely with simple sensors and calibrated periodically with more rigorous measurements. This empirical algorithm provides a simple and practical solution that would allow small-hold aquaculture operators and government officials to expand monitoring effort and data coverage to improve GHG assessment.

Declaration of Competing Interest

The authors declare that they have no known competing financial interests or personal relationships that could have appeared to influence the work reported in this paper.

Acknowledgements

The study received collaborative financial support from the National Science Foundation of Fujian Province, China (No. 2022R1002006, and No. 2020J01136) and the National Natural Science Foundation of China (No. 41801070, and No. 41671088).

Data availability

Data will be made available on request.

References

Avnimelech, Y., Ritvo, G., 2003. Shrimp and fish pond soils: processes and management. Aquaculture 220, 549–567. https://doi.org/10.1016/S0044-8486(02)00641-5.

Bastviken, D., Cole, J.J., Pace, M.L., Van de Bogert, M.C., 2008. Fates of methane from different lake habitats: Connecting whole-lake budgets and CH4 emissions. J. Geophys. Res.-Biogeo. 113, G02024. https://doi.org/10.1029/2007JG000608.

Bastviken, D., Tranvik, L.J., Downing, J.A., Crill, P.M., Enrich-Prast, A., 2011. Freshwater methane emissions offset the continental carbon sink. Science 331, 50. https://doi.org/10.1126/science.1196808.

Berberich, M.E., Beaulieu, J.J., Hamilton, T.L., Waldo, S., Buffam, I., 2020. Spatial variability of sediment methane production and methanogen communities within a eutrophic reservoir: Importance of organic matter source and quantity. Limnol. Oceanogr. 65 (6), 1336–1358. https://doi.org/10.1002/lno.11392.

Bernhard, A.E., Peele, E.R., 1997. Nitrogen limitation of phytoplankton in a shallow embayment in northern Puget Sound. Estuar. Coast. 20 (4), 759–769. https://doi. org/10.2307/1352249.

Bogard, M.J., del Giorgio, P.A., Boutet, L., Chaves, M.C.G., Prairie, Y.T., Merante, A., Derry, A.M., 2014. Oxic water column methanogenesis as a major component of aquatic CH4 fluxes. Nat. Commun. 5, 5350. https://doi.org/10.1038/ncomms6350.

Borges, A.V., Darchambeau, F., Lambert, T., Bouillon, S., Morana, C., Brouy`ere, S., Hakoun, V., Jurado, A., Tseng, H.-C., Descy, J.-P., Roland, F.A.E., 2018. Effects of agricultural land use on fluvial carbon dioxide, methane and nitrous oxide concentrations in a large European river, the Meuse Belgium. Sci. Total Environ. 610–611, 342–355. https://doi.org/10.1016/j.scitotenv.2017.08.047.

Borges, A.V., Darchambeau, F., Teodoru, C.R., Marwick, T.R., Tamooh, F., Geeraert, N., Omengo, F.O., Gu´erin, F., Lambert, T., Morana, C., Okuku, E., Bouillon, S., 2015. Globally significant greenhouse-gas emissions from African inland waters. Nat. Geosci. 8, 637–642. https://doi.org/10.1038/NGEO2486.

Boyd, C.E., Wesley Wood, C., Chaney, P.L., Queiroz, J.F., 2010. Role of aquaculture pond sediments in sequestration of annual global carbon emissions. Environ. Pollut. 158, 2537–2540. https://doi.org/10.1016/j.envpol.2010.04.025.

Chambers, L.G., Osborne, T.Z., Reddy, K.R., 2013. Effect of salinity-altering pulsing events on soil organic carbon loss along an intertidal wetlands gradient: a laboratory experiment. Biogeochemistry 115, 363–383. https://doi.org/10.1007/s10533-013- 9841-5.

Chanda, A., Das, S., Bhattacharyya, S., Das, I., Giri, S., Mukhopadhyay, A., Samanta, S., Dutta, D., Akhand, A., Choudhury, S.B., Hazra, S., 2019. CO2 fluxes from aquaculture ponds of a tropical wetland: Potential of multiple lime treatment in reduction of CO2 emission. Sci. Total Environ. 655, 1321–1333. https://doi.org/10.1016/j. scitotenv.2018.11.332.

Chen, Y., Dong, S.L., Wang, Z.N., Wang, F., Gao, Q.F., Tian, X.L., Xiong, Y.H., 2015. Variations in CO2 fluxes from grass carp Ctenopharyngodon idella aquaculture polyculture ponds. Aquacult. Env. Interac. 8, 31–40. https://doi.org/10.3354/ aei00149.

Chen, Y., Dong, S.L., Wang, F., Gao, Q.F., Tian, X.L., 2016. Carbon dioxide and methane fluxes from feeding and no-feeding mariculture ponds. Environ. Pollut. 212, 489–497. https://doi.org/10.1016/j.envpol.2016.02.039.

Chen, G.Z., Bai, J.H., Bi, C., Wang, Y.Q., Cui, B.S., 2023. Global greenhouse gas emissions from aquaculture: a bibliometric analysis. Agr. Ecosyst. Environ. 348, 108405 https://doi.org/10.1016/j.agee.2023.108405.

Chowdhury, T.R., Dick, R.P., 2013. Ecology of aerobic methanotrophs in controlling methane fluxes from wetlands. Appl. Soil Ecol. 65, 8–22. https://doi.org/10.1016/j.apsoil.2012.12.014.

Cotovicz Jr., L.C., Knoppers, B.A., Brandini, N., Poirier, D., Costa Santos, S.J., Abril, G., 2016. Spatio-temporal variability of methane (CH4) concentrations and diffusive fluxes from a tropical coastal embayment surrounded by a large urban area (Guanabara Bay, Rio de Janeiro, Brazil). Limnol. Oceanogr. 61 (S1), S238–S252.https://doi.org/10.1002/lno.10298.

Cole, J.J., Caraco, N.F., 1998. Atmospheric exchange of carbon dioxide in a low-wind oligotrophic lake measured by the addition of SF6. Limnol. Oceanogr. 43 (4), 647–656. https://doi.org/10.4319/lo.1998.43.4.0647.

Crusius, J., Wanninkhof, R., 2003. Gas transfer velocities measured at low wind speed over a lake. Limnol. Oceanogr. 48 (3), 1010–1017.

Davidson, T.A., Audet, J., Jeppesen, E., Landkildehus, F., Lauridsen, T.L., Søndergaard, M., Syv¨aranta, J., 2018. Synergy between nutrients and warming enhances methane ebullition from experimental lakes. Nat. Clim. Change 8 (2),156. https://doi.org/10.1038/s41558-017-0063-z.

Deemer, B.R., Harrison, J.A., Li, S.Y., Beaulieu, J.J., Delsontro, T., Barros, N., BezerraNeto, J.F., Powers, S.M., Santos, M.A.D., Vonk, J.A., 2016. Greenhouse gas emissions from reservoir water surfaces: a new global synthesis. Bioscience 66, 949–964. https://doi.org/10.1093/biosci/biw117.

de Mello, N.A.S.T., Brighenti, L.S., Barbosa, F.A.R., Staehr, P.A., Bezerra Neto, J.F., 2018. Spatial variability of methane (CH4) ebullition in a tropical hypereutrophic reservoir: silted areas as a bubble hot spot. Lake Reserv. Manage. 34 (2), 105–114. https://doi.org/10.1080/10402381.2017.1390018.

Dong, Y.H., Yuan, J.J., Li, J.J., Liu, D.Y., Qiu, Y., Zhang, X., Xiang, J., Ding, W.X., 2023a. Conversion of natural coastal wetlands to mariculture ponds dramatically decreased methane production by reducing substrate availability. Agr. Ecosyst. Environ. 356, 108646 https://doi.org/10.1016/j.agee.2023.108646.

Dong, B.G., Xi, Y., Cui, Y.X., Peng, S.S., 2023b. Quantifying methane emissions from aquaculture ponds in China. Environ. Sci. Technol. 57 (4), 1576–1583. https://doi.org/10.1021/acs.est.2c05218.

Downing, J.A., 2010. Emerging global role of small lakes and ponds: little things mean a lot. Limnetica 29, 9–23. https://doi.org/10.1899/09-028.1.

Duan, Y.Q., Li, X., Zhang, L.P., Chen, D., Liu, S.A., Ji, H.Y., 2020. Mapping national-scale aquaculture ponds based on the Google Earth Engine in the Chinese coastal zone. Aquaculture 520, 734666. https://doi.org/10.1016/j.aquaculture.2019.734666.

FAO, 2017. Fishery and aquaculture statistics (global aquaculture production 1950–2014). FishStatJ. http://www.fao.org/fishery/statistics/software/fishstatj/en.

FAO, 2020. The State of World Fisheries and Aquaculture 2020. Sustainability in action. Rome. https://doi.org/10.4060/ca9229en.

Fang, X.T., Wang, C., Zhang, T.R., Zheng, F.W., Zhao, J.T., Wu, S., Barthel, M., Six, J., Zou, J.W., Liu, S.W., 2022. Ebullitive CH4 flux and its mitigation potential by aeration in freshwater aquaculture: Measurements and global data synthesis. Agr. Ecosyst. Environ. 335, 108016 https://doi.org/10.1016/j.agee.2022.108016.

Flickinger, D.L., Costa, G.A., Dantas, D.P., Proença, D.C., David, F.S., Durborow, R.M., Moraes-Valentia, P., Valenti, W.C., 2020. The budget of carbon in the farming of the Amazon river prawn and tambaqui fish in earthen pond monoculture and integrated multitrophic systems. Aquacult. Rep. 17, 100340 https://doi.org/10.1016/j.aqrep.2020.100340.

Friedlingstein, P., O'Sullivan, M., Jones, M.W., Andrew, R.M., Gregor, L., et al., 2022. Global Carbon Budget 2022. Earth Syst. Sci. Data 14, 4811–4900. https://doi.org/10.5194/essd-14-4811-2022.

Gao, D.Z., Liu, M., Hou, L.J., Lai, D.Y.F., Wang, W.Q., Li, X.F., Zeng, A.Y., Zheng, Y.L., Han, P., Yang, Y., Yin, G.Y., 2019. Effects of shrimp-aquaculture reclamation on sediment nitrate dissimilatory reduction processes in a coastal wetland of southeastern China. Environ. Pollut. 255, 113219 https://doi.org/10.1016/j.envpol.2019.113219.

Gruca-Rokosz, R., Szal, D., Bartoszek, L., Pękala, A., 2020. Isotopic evidence for vertical diversification of methane production pathways in freshwater sediments of Nielisz reservoir (Poland). Catena 195, 104803. https://doi.org/10.1016/j.catena.2020.104803.

Gudasz, C., Bastviken, D., Steger, K., Premke, K., Sobek, S., Tranvik, L.J., 2010. Temperature-controlled organic carbon mineralization in lake sediments. Nature 466, 478–482. https://doi.org/10.1038/nature09186.

Holgerson, M.A., 2015. Drivers of carbon dioxide and methane supersaturation in small, temporary ponds. Biogeochemistry 124 (1–3), 305–318. https://doi.org/10.1007/s10533-015-0099-y.

Holgerson, M.A., Raymond, P.A., 2016. Large contribution to inland water CO2 and CH4 emissions from very small ponds. Nat. Geosci. 9 (3), 222–226. https://doi.org/10.1038/ngeo2654.

Hu, B.B., Xu, X.F., Zhang, J.F., Wang, T.L., Meng, W.Q., Wang, D.Q., 2020. Diurnal variations of greenhouse gases emissions from reclamation mariculture ponds. Estuar. Coast. Shelf S. 237, 106677 https://doi.org/10.1016/j.ecss.2020.106677.

Huttunen, J.T., Alm, J., Liikanen, A., Juutinen, S., Larmola, T., Hammar, T., Silvola, J., Martikainen, P.J., 2003. Fluxes of methane, carbon dioxide and nitrous oxide in boreal lakes and potential anthropogenic effects on the aquatic greenhouse gas emissions. Chemosphere 52, 609–621. https://doi.org/10.1016/s0045-6535(03)00243-1.

IPCC, 2019 (Eds.). In: Calvo Buendia, E., Tanabe, K., Kranjc, A., Baasansuren, J., Fukuda, M., Ngarize, S. (Eds.), 2019 Refinement to the 2006 IPCC Guidelines for National Greenhouse Gas Inventories, Volume 4. IPCC, Switzerland. Kanagawa, Japan. Chapter 07.

Jensen, S.A., Webb, J.R., Simpson, G.L., Baulch, H.M., Leavitt, P.R., Finlay, K., 2023. Differential controls of greenhouse gas (CO2, CH4, and N2O) concentrations in natural and constructed agricultural waterbodies on the Northern Great Plains. J. Geophys. Res.-Biogeo. 128, e2022JG007261 https://doi.org/10.1029/ 2022JG007261.

Jia, J.J., Sun, K., Lü, S.D., Li, M.X., Wang, Y.F., Yu, G.R., Gao, Y., 2022. Determining whether Qinghai–Tibet Plateau waterbodies have acted like carbon sinks or sources over the past 20 years. Sci. Bull. 67, 2345–2357. https://doi.org/10.1016/j. scib.2022.10.023.

Kang, L.J., Zhu, G.W., Zhu, M.Y., Xu, H., Zou, W., Xiao, M., Zhang, Y.L., Qin, B.Q., 2023. Bloom-induced internal release controlling phosphorus dynamics in large shallow eutrophic Lake Taihu. China. Environ. Res. 231 (Part 3), 116251 https://doi.org/ 10.1016/j.envres.2023.116251.

Kosten, S., Almeida, R.M., Barbosa, I., Mendonç, R., Muzitano, I.S., Oliveira-Junior, E.S., Vroom, R.J.E., Wang, H.J., Barros, N., 2020. Better assessments of greenhouse gas emissions from global fish ponds needed to adequately evaluate aquaculture footprint. Sci. Total Environ 748, 141247. https://doi.org/10.1016/j. scitotenv.2020.141247.

Lapointe, B.E., Herren, L.W., Debortoli, D.D., Vogel, M.A., 2015. Evidence of sewagedriven eutrophication and harmful algal blooms in Florida's Indian River Lagoon. Harmful Algae 43, 82–102. https://doi.org/10.1016/j.hal.2015.01.004.

Le Qu´er´e, C., Andrew, R.M., Friedlingstein, P., Sitch, S., Hauck, J., et al., 2018. Global Carbon Budget 2018. Earth Syst. Sci. Data 10, 2141–2194. https://doi.org/10.5194/ essd-10-2141-2018.

Li, S.Y., Bush, R.T., Santos, I.R., Zhang, Q.F., Song, K.S., Mao, R., Wen, Z.D., Lu, X.X., 2018. Large greenhouse gases emissions from China's lakes and reservoirs. Water Res 147, 13–24. https://doi.org/10.1016/j.watres.2018.09.053.

Lin, G.M., Lin, X.B., 2022. Bait input altered microbial community structure and increased greenhouse gases production in coastal wetland sediment. Water Res 218, 118520. https://doi.org/10.1016/j.watres.2022.118520.

Liu, S.W., Hu, Z.Q., Wu, S., Li, S.Q., Li, Z.F., Zou, J.W., 2016. Methane and nitrous oxide emissions reduced following conversion of rice paddies to inland crab-fish aquaculture in southeast. China. Environ. Sci. Technol. 50 (2), 633–642. https://doi. org/10.1021/acs.est.5b04343.

Liu, Z.H., Dreybrodt, W., Wang, H.J., 2010. A new direction in effective accounting for the atmospheric CO2 budget: considering the combined action of carbonate dissolution, the global water cycle and photosynthetic uptake of DIC by aquatic organisms. Earth Sci. Rev. 99, 162–172. https://doi.org/10.1016/j. earscirev.2010.03.001.

Luo, J.H., Sun, Z., Lu, L.R., Xiong, Z.Y., Cui, L.P., Mao, Z.G., 2022. Rapid expansion of coastal aquaculture ponds in Southeast Asia: Patterns, drivers and impacts. J. Environ. Manage. 315, 115100 https://doi.org/10.1016/j.jenvman.2022.115100.

MacLeod, M.J., Hasan, M.R., Robb, D.H., Mamun-Ur-Rashid, M., 2020. Quantifying greenhouse gas emissions from global aquaculture. Sci. Rep. 10 (1), 11679. https:// doi.org/10.1038/s41598-020-68231-8.

Martinez, D., Anderson, M.A., 2013. Methane production and ebullition in a shallow, artificially aerated, eutrophic temperate lake (Lake Elsinore, CA). Sci. Total Environ. 454, 457–465. https://doi.org/10.1016/j.scitotenv.2013.03.040.

Marescaux, A., Thieu, V., Garnier, J., 2018. Carbon dioxide, methane and nitrous oxide emissions from the human-impacted Seine watershed in France. Sci. Total Environ. 643, 247–259. https://doi.org/10.1016/j.scitotenv.2018.06.151.

Molnar, N., Welsh, D.T., Marchand, C., Deborde, J., Meziane, T., 2013. Impacts of shrimp farm effluent on water quality, benthic metabolism and N-dynamics in a mangrove forest (New Caledonia). Estuar. Coast. Shelf S. 117, 12–21. https://doi.org/10.1016/ j.ecss.2012.07.012.

Musenze, R.S., Grinham, A., Werner, U., Gale, D., Sturm, K., Udy, J., Yuan, Z.G., 2014. Assessing the spatial and temporal variability of diffusive methane and nitrous oxide emissions from subtropical freshwater reservoirs. Environ. Sci. Technol. 48, 14499–14507. https://doi.org/10.1021/es505324h.

Myhre, G., Shindell, D., Breon, F.M., Collins, W., Fuglestvedt, J., Huang, J., Koch, D., Lamarque, J.F., Lee, D., Mendoza, B., Nakajima, T., Robock, A., Stephens, G., Takemura, T., Zhang, H., 2013. Anthropogenic and natural radiative forcing. In: climate change 2013, the physical science basis. Contribution of working group i to the fifth assessment report of the intergovernmental panel on climate change. Cambridge University Press, Cambridge.

Natchimuthu, S., Sundgren, I., Gålfalk, M., Klemedtsson, L., Crill, P., Danielsson, Å., Bastviken, D., 2016. Spatio-temporal variability of lake CH4 fluxes and its influence on annual whole lake emission estimates. Limnol. Oceanogr. 61 (S1), S13–S26. https://doi.org/10.1002/lno.10222.

National Oceanic and Atmospheric (NOAA), 2023. Carbon cycle greenhouse gases. Available in: https://www.esrl.noaa.gov/gmd/ccgg/.

Naylor, R.L., Hardy, R.W., Buschmann, A.H., Bush, S.R., Cao, L., Klinger, D.H., Little, D. C., Lubchenco, J., Shumway, S.E., Troell, M., 2021. A 20-year retrospective review of global aquaculture. Nature 591, 551–563. https://doi.org/10.1038/s41586-021-03308-6.

Neubauer, S.C., Franklin, R.B., Berrier, D.J., 2013. Saltwater intrusion into tidal freshwater marshes alters the biogeochemical processing of organic carbon. Biogeosciences 10, 8171–8183. https://doi.org/10.5194/bg-10-8171-2013.

Neubauer, S.C., Megonigal, J.P., 2019. Correction to: Moving beyond global warming potentials to quantify the climatic role of ecosystems. Ecosystems 22, 1931–1932. https://doi.org/10.1007/s10021-019-00422-5.

Peacock, M., Audet, J., Bastviken, D., Cook, S., Futter, M.N., 2021. Small artificial waterbodies are widespread and persistent emitters of methane and carbon dioxide. Global Change Biol 27, 5109–5123. https://doi.org/10.1111/gcb.15762.

Poffenbarger, H.J., Needelman, B.A., Megonigal, J.P., 2011. Salinity influence on methane emissions from tidal marshes. Wetlands 31, 831–842. https://doi.org/10.1007/s13157-011-0197-0.

Pouil, S., Samsudin, R., Slembrouck, J., Sihabuddin, A., Sundari, G., Khazaidan, K., Kristanto, A.H., Pantjara, B., Caruso, D., 2019. Nutrient budgets in a small-scale freshwater fish pond system in Indonesia. Aquaculture 504, 267–274. https://doi.org/10.1016/j.aquaculture.2019.01.067.

Praetzel, L.S.E., Schmiedeskamp, M., Knorr, K.H., 2021. Temperature and sediment properties drive spatiotemporal variability of methane ebullition in a small and shallow temperate lake. Limnol. Oceanogr. 66 (7), 2598–2610. https://doi.org/10.1002/lno.11775.

Pr˙eskienis, V., Laurion, I., Bouchard, F., Douglas, P.M.J., Billett, M.F., Fortier, D., Xu, X. M., 2021. Seasonal patterns in greenhouse gas emissions from lakes and ponds in a High Arctic polygonal landscape. Limnol. Oceanogr. 66, S117–S141. https://doi.org/10.1002/lno.11660.

Raymond, P.A., Hartmann, J., Lauerwald, R., Sobek, S., McDonald, C., Hoover, M., Butman, D., Striegl, R., Mayorga, E., Humborg, C., Kortelainen, P., Duerr, H., Meybeck, M., Ciais, P., Guth, P., 2013. Global carbon dioxide emissions from inland waters. Nature 503 (7476), 355–359. https://doi.org/10.1038/nature12760.

Rubbo, M., Cole, J., Kiesecker, J., 2006. Terrestrial subsidies of organic carbon support net ecosystem production in temporary forest ponds: evidence from an ecosystem experiment. Ecosystems 9, 1170–1176. https://doi.org/10.1007/s10021-005-0009-6.

Sahu, B.C., Adhikari, S., Mahapatra, A.S., Dey, L., 2013. Carbon, nitrogen, and phosphorus budget in scampi (Macrobrachium rosenbergii) culture ponds. Environ. Monit. Assess. 185, 10157–10166. https://doi.org/10.1007/s10661-013-3320-2.

Segarra, K.E.A., Comerford, C., Slaughter, J., Joye, S.B., 2013. Impact of electron acceptor availability on the anaerobic oxidation of methane in coastal freshwater and brackish wetland sediments. Geochimi. Cosmochimi. Ac. 115, 15–30. https://doi.org/10.1016/j.gca.2013.03.029.

Segers, R., 1998. Methane production and methane consumption: a review of processes underlying wetland methane fluxes. Biogeochemistry 41, 23–51. https://doi.org/10.1023/A:1005929032764.

Schrier-Uijl, A.P., Veraart, A.J., Leffelaar, P.A., Berendse, F., Veenendaal, E.M., 2011. Release of CO2 and CH4 from lakes and drainage ditches in temperate wetlands. Biogeochemistry 102 (1-3), 265–279. https://doi.org/10.1007/s10533-010-9440-7.

Tan, L.S., Ge, Z.M., Ji, Y.H., Lai, D.Y.F., Temmerman, S., Li, S.H., Li, X.Z., Tang, J.W., 2022. Land use and land cover changes in coastal and inland wetlands cause soil carbon and nitrogen loss. Global Ecol. Biogeogr. 31, 2541–2563. https://doi.org/10.1111/geb.13597.

Tan, L.S., Zhang, L.H., Yang, P., Tong, C., Lai, D.Y.F., Yang, H., Hong, Y., Tian, Y.L., Tang, C., Ruan, M.J., Tang, K.W., 2023. Effects of conversion of coastal marshes to aquaculture ponds on sediment anaerobic CO2 production and emission in a subtropical estuary of China. J. Environ. Manage. 338, 117813 https://doi.org/10.1016/j.jenvman.2023.117813.

Tang, K.W., McGinnis, D.F., Ionescu, D., Grossart, H.-P., 2016. Methane production in oxic lake waters potentially increases aquatic methane flux to air. Environ. Sci. Technol. Lett. 3 (6), 227–233. https://doi.org/10.1021/acs.estlett.6b00150.

Tian, Y.L, Yang, P., Yang, H., Wang, H.M., Zhang, L.H., Tong, C., Lai, D.Y.F., Lin, Y.X., Tan, L.S., Hong, Y., Tang, C., Tang, K.W., 2023. Diffusive nitrous oxide (N2O) fluxes across the sediment-water-atmosphere interfaces in aquaculture shrimp ponds in a subtropical estuary: Implications for climate warming. Agr. Ecosyst. Environ. 341, 108218 https://doi.org/10.1016/j.agee.2022.108218.

Tong, C., Morris, J.T., Huang, J.F., Xu, H., Wan, S.A., 2018. Changes in pore-water chemistry and methane emission following the invasion of *Spartina alterniflora* into an oliogohaline marsh. Limnol. Oceanogr. 63, 384–396. https://doi.org/10.1002/ lno.10637.

Tong, C., Bastviken, D., Tang, K.W., Yang, P., Yang, H., Zhang, Y.F., Guo, Q.Q., Lai, D.Y. F., 2020. Annual CO2 and CH4 fluxes in coastal earthen ponds with *Litopenaeus vannamei* in southeastern China. Aquaculture 545, 737229. https://doi.org/ 10.1016/j.aquaculture.2021.737229.

Vizza, C., West, W.E., Jones, S.E., Hart, J.A., Lamberti, G.A., 2017. Regulators of coastal wetland methane production and responses to simulated global change. Biogeosciences 14 (2), 431–446. https://doi.org/10.5194/bg-14-431-2017.

Wang, F.S., Lang, Y.C., Liu, C.Q., Qin, Y., Yu, N.X., Wang, B.L., 2019. Flux of organic carbon burial and carbon emission from a large reservoir: implications for the cleanliness assessment of hydropower. Sci. Bull. 64, 603–611. https://doi.org/ 10.1016/j.scib.2019.03.034.

Wang, J., Feng, L., Palmer, P.I., Liu, Y., Fang, S., Bsch, H., O'Dell, C.W., Tang, X.P., Yang, D.X., Liu, L.X., Xia, C.Z., 2020. Large Chinese land carbon sink estimated from atmospheric carbon dioxide data. Nature 586, 720–723. https://doi.org/10.1038/ s41586-020-2849-9.

Wanninkhof, R., 1992. Relationship between wind-speed and gas-exchange over the ocean. J. Geophys. Res.-Oceans 97, 7373–7382. https://doi.org/10.1029/ 92jc00188.

Welti, N., Hayes, M., Lockington, D., 2017. Seasonal nitrous oxide and methane emissions across a subtropical estuarine salinity gradient. Biogeochemistry 132 (1- 2), 55–69. https://doi.org/10.1007/s10533-016-0287-4.

Wilson, B.J., Mortazavi, B., Kiene, R.P., 2015. Spatial and temporal variability in carbon dioxide and methane exchange at three coastal marshes along a salinity gradient in a northern Gulf of Mexico estuary. Biogeochemistry 123 (3), 329–347. https://doi. org/10.1007/s10533-015-0085-4.

Xiao, Q.T., Duan, H.T., Qi, T.C., Hu, Z.H., Liu, S.D., Zhang, M., Lee, X.H., 2020. Environmental investments decreased partial pressure of CO2 in a small eutrophic urban lake: Evidence from long-term measurements. Environ. Pollut. 263, 114433 https://doi.org/10.1016/j.envpol.2020.114433.

Xu, H., Paerl, H.W., Zhu, G.W., Qin, B.Q., Hall, N.S., Zhu, M.Y., 2017. Long-term nutrient trends and harmful cyanobacterial bloom potential in hypertrophic Lake Taihu. China. Hydrobiologia 787, 229–242. https://doi.org/10.1007/s10750-016-2967-4.

Yang, G.B., Zheng, Z.H., Abbott, B.W., Olefeldt, D., Knoblauch, C., Song, Y.T., Kang, L.Y., Qin, S.Q., Peng, Y.F., Yang, Y.H., 2023a. Characteristics of methane emissions from alpine thermokarst lakes on the Tibetan Plateau. Nat. Commun. 14, 3121. https:// doi.org/10.1038/s41467-023-38907-6.

Yang, H., Huang, X., Hu, J., Thompson, J.R., Flower, R.J., 2022a. Achievements, challenges and global implications of China's carbon neutral pledge. Front. Env. Sci. Eng. 16 (8), 111. https://doi.org/10.1007/s11783-022-1532-9.

Yang, P., Yang, H., Sardans, J., Tong, C., Zhao, G.H., Pe˜nuelas, J., Li, Ling, Zhang, Y.F., Tan, L.S., Chun, K.P., Lai, D.Y.F., 2020a. Large spatial variations in diffusive CH4 fluxes from a subtropical coastal reservoir affected by sewage discharge in southeast China. Environ. Sci. Technol. 54 (22), 14192–14203. https://doi.org/10.1021/acs. est.0c03431.

Yang, P., Zhang, Y.F., Yang, H., Guo, Q.Q., Lai, D.Y.F., Zhao, G.H., Li, L., Tong, C., 2020b. Ebullition was a major pathway of methane emissions from the aquaculture ponds in southeast China. Water Res 184, 116176. https://doi.org/10.1016/j. watres.2020.116176.

Yang, P., Lai, D.Y.F., Yang, H., Lin, Y.X., Tong, C., Hong, Y., Tian, Y.L., Tang, C., Tang, K. W., 2022b. Large increase in CH4 emission following conversion of coastal marsh to aquaculture ponds caused by changing gas transport pathways. Water Res 222, 118882. https://doi.org/10.1016/j.watres.2022.118882.

Yang, P., Lai, D.Y.F., Yang, H., Tong, C., 2019. Carbon dioxide dynamics from sediment, sediment-water interface and overlying water in the aquaculture shrimp ponds in subtropical estuaries, southeast. China. J. Environ. Manage. 236, 224–235. https:// doi.org/10.1016/j.jenvman.2019.01.088.

Yang, P., Tang, K.W., Yang, H., Tong, C., Zhang, L.H., Lai, D.Y.F., Hong, Y., Tan, L.S., Zhu, W.Y., Tang, C., 2023b. Contrasting effects of aeration on methane (CH4) and nitrous oxide (N2O) emissions from subtropical aquaculture ponds and implications for global warming mitigation. J. Hydrol. 617, 128876 https://doi.org/10.1016/j. jhydrol.2022.128876.

Yuan, J.J., Xiang, J., Liu, D.Y., Kang, H., He, T.H., Kim, S., Lin, Y.X., Freeman, C., Ding, W.X., 2019. Rapid growth in greenhouse gas emissions from the adoption of industrial-scale aquaculture. Nat. Clim. Change 9 (4), 318–322. https://doi.org/ 10.1038/s41558-019-0425-9.

Yuan, J.J., Liu, D.Y., Xiang, J., He, T.H., Kang, H., Ding, W.X., 2021. Methane and nitrous oxide have separated production zones and distinct emission pathways in freshwater aquaculture ponds. Water Res 190, 116739. https://doi.org/10.1016/j. watres.2020.116739.

Zabranska, J., Pokorna, D., 2018. Bioconversion of carbon dioxide to methane using hydrogen and hydrogenotrophic methanogens. Biotechnol. Adv. 36 (3), 707–720. https://doi.org/10.1016/j.biotechadv.2017.12.003.

Zhang, K., Xie, J., Yu, D.G., Wang, G.J., Yu, E.M., Gong, W.B., Li, Z.F., Wang, C.C., Xia, Y., 2018. A comparative study on the budget of nitrogen and phosphorus in polyculture systems of snakehead with bighead carp. Aquaculture 483, 69–75. https://doi.org/10.1016/j.aquaculture.2017.10.004.

Zhang, Y.F., Lyu, M., Yang, P., Lai, D.Y.F., Tong, C., Zhao, G.H., Li, L., Zhang, Y.H., Yang, H., 2021. Spatial variations in CO2 fluxes in a subtropical coastal reservoir of Southeast China were related to urbanization and land-use types. J. Environ. Sci. 109, 206–218. https://doi.org/10.1016/j.jes.2021.04.003.

Zhang, Y.P., Qin, Z.C., Li, TT., Zhu, X.D., 2022. Carbon dioxide uptake overrides methane emission at the air-water interface of algae-shellfish mariculture ponds: Evidence from eddy covariance observations. Sci. Total Environ. 815, 152867 https://doi.org/ 10.1016/j.scitotenv.2021.152867.

Zhao, J.Y., Zhang, M., Xiao, W., Jia, L., Zhang, X.F., Wang, J., Zhang, Z., Xie, Y.H., Pu, Y. N., Liu, S.D., Feng, Z.Z., Lee, X.H., 2021. Large methane emission from freshwater aquaculture ponds revealed by long-term eddy covariance observation. Agr. Forest. Meteorol. 108600, 308–309. https://doi.org/10.1016/j.agrformet.2021.108600.

Zhou, Y.Q., Xiao, Q.T., Yao, X.L., Zhang, Y.L., Zhang, M., Shi, K., Lee, X.H., Podgorski, D. C., Qin, B.Q., Spencer, R.G.M., Jeppesen, E., 2018. Accumulation of terrestrial dissolved organic matter

potentially enhances dissolved methane levels in eutrophic Lake Taihu. China. Environ. Sci. Technol. 52 (18), 10297–10306. https://doi.org/ 10.1021/acs.est.8b02163.

Zosel, J., Oelßner, W., Decker, M., Gerlach, G., Guth, U., 2011. The measurement of dissolved and gaseous carbon dioxide concentration. Meas. Sci. Technol. 22 (7), 072001 https://doi.org/10.1088/0957-0233/22/7/072001.